Prev. Nutr. Food Sci. 2024;29(4):533-545
https://doi.org/10.3746/pnf.2024.29.4.533
ISSN 2287-8602

# Inhibition of Differentiation of 3T3-L1 Cells by Increasing Glioma-Associated Oncogene Expression in *Chrysanthemum indicum* L. Using *Lactococcus lactis* KCTC 3115

**Young-Jae Cho[1]*, Ja-Bok Lee[1]*, Yunjung Lee[2], Min Soo Lee[3], and Jaeyoung Choi[3]**

[1]LFOUNDER Inc., Incheon 21984, Korea
[2]Department of Hotel & Foodservice Culinary Art, JEI University, Incheon 22573, Korea
[3]Department of Culinary Arts & Hotel Food Service, Yeonsung University, Gyeonggi 14011, Korea

**ABSTRACT:** The inhibitory effect of *Chrysanthemum indicum* L. on adipocyte differentiation can be enhanced by lactic acid bacteria (LAB) fermentation. In this study, we assessed the cellulose resolution, *C. indicum* L. quantity, and fermentation time and process to verify the LAB selection and fermentation efficiency. In addition, the antioxidant activity, adipocyte signaling and differentiation, and hedgehog (Hh) signaling were investigated, and the changes in compounds before and after fermentation were determined by ultra-high performance liquid chromatography (UHPLC). All strains exhibited satisfactory cellulose resolution. With 20% *C. indicum* L., fermentation was only effective up to 24 h. The results of the antioxidant assays showed that the 2,2-diphenyl-1-picrylhydrazyl and 2,2'-azino-bis(3-ethylbenzothiazoline-6-sulfonate) radical scavenging capacities were higher in all fermentations than in unfermented *C. indicum* L. extract (CI). 3T3-L1 cell differentiation signaling evaluation revealed that CI inhibited adipocyte differentiation by reducing peroxisome proliferator-activated receptor-γ, CCAAT/enhancer binding protein-α, and phosphorylated AMP-activated protein kinase activity in all fermentations. In the Hh signaling analysis, CI fermented with *Lactococcus lactis* KCTC 3115 significantly increased glioma-associated oncogene 1 (GLI1) activity by inhibiting patched 1 activity and activating smoothened ($P<0.001$). UHPLC quantitative analysis revealed elevated levels of luteolin and quercetin. Fermentation with *C. indicum* L. and *L. lactis* KCTC 3115 activated GLI1, a transcription factor in the Hh signaling pathway, which enhanced the inhibition of adipocyte differentiation, indicating its potential in anti-obesity treatment. However, the exact compounds affecting GLI1 activity require further elucidation in future studies.

**Keywords:** adipocytes, *Chrysanthemum indicum* L., fermentation, GLI1, *Lactococcus lactis* KCTC 3115

## INTRODUCTION

Adipogenesis involves the differentiation of undifferentiated progenitor cells into adipocytes. Adipocyte differentiation is driven by proteins in the CCAAT/enhancer binding protein (C/EBP) family. This family comprises three member proteins: CCAAT/enhancer binding protein-α (C/EBPα), CCAAT/enhancer binding protein-β (C/EBPβ), and CCAAT/enhancer binding protein-δ (C/EBPδ) (Jemai et al., 2020). In addition to the C/EBP proteins, several other transcription factors are involved in adipogenesis, including the nuclear hormone receptor peroxisome proliferator-activated receptor (PPAR) and adipocyte determination and differentiation factor 1/sterol regulatory element binding protein-1c, which is a member of the basic helix-loop-helix family (Moldes et al., 1999; Nerurkar et al., 2010). Increased expression of C/EBPβ and C/EBPδ induces early adipocyte differentiation and increases the expression of other factors, including peroxisome proliferator-activated receptor-γ (PPARγ). Upregulated PPARγ induces C/EBPα expression, which drives late adipocyte differentiation and contributes to intracellular fat accumulation (Darlington et al., 1998; Rosen and MacDougald, 2006). These transcription factors have therefore been the primary targets of adipogenesis inhibition studies using 3T3-L1 and 3T3-F442A cells (Rosen et al., 2002).

Hedgehog (Hh) signaling, first discovered in fruit flies, involves the transmission of signals from the cell membrane to the nucleus. Hh signaling occurs during normal embryonic development in vertebrates and during tissue

Received 21 August 2024; Revised 21 September 2024; Accepted 25 September 2024; Published online 31 December 2024

Correspondence to Jaeyoung Choi, E-mail: juynay@yeonsung.ac.kr
*These authors contributed equally to this work.

and organ development in the body. Hh signaling is normally inactive in adult cells but becomes activated to heal and repair body tissues. Activated Hh signaling is crucial for maintaining somatic stem cells, pluripotent cells, and some epithelial cells, leading to cell regeneration in various tissues (Skoda et al., 2018). Adipocytes are also affected by Hh signaling, and there is growing interest in Hh signaling as a target for obesity treatment, as Hh signaling has been found to be able to reduce fat accumulation in 3T3-L1 cells (Cousin et al., 2007).

Three ligands are involved in Hh signaling: sonic hedgehog (SHh), Indian hedgehog, and desert hedgehog. SHh is the most common of these three. Hh signaling involves the patched (PTCH) protein, a 12-transmembrane protein that binds ligands, and the smoothened (SMO) protein, a 7-transmembrane protein with G-protein receptors that act as signal transducers. PTCH has two isoforms: Patched 1 (PTCH1) and patched 2, and the former is critical in Hh signaling (Hu et al., 2015). When SMO is activated by PTCH1, it translocates glioma-associated oncogene 1 (GLI1), glioma-associated oncogene 2 (GLI2), and glioma-associated oncogene 3 (GLI3), which are cleaved from the suppressor of fusion (SUFU), into the cell nucleus to promote the transcription of target genes (Zhang et al., 2024). Among the three GLI proteins, GLI1 appears to be a key mediator of Hh signaling (Zhou et al., 2022). Adipocyte progenitors maintain an activated state of Hh signaling, but when they differentiate into adipocytes, Hh signaling switches to an inactive state to regulate differentiation (Fan et al., 2018). Among the transcription factors involved in adipocyte differentiation, C/EBPα and PPARγ have been reported to be regulated by the GLI1 protein (Chen et al., 2018).

In our previous anti-obesity study, we reported that enzymatically treated *Chrysanthemum indicum* L. extract (CI) reduced the expression and serum levels of the adipogenesis-related transcription factors, PPARγ and C/EBPα, in high-fat diet (HFD)-induced obese mice (Lee et al., 2019). The phenolic compounds of *C. indicum* L. were found to contain >190 chemical constituents. These included luteolin, apigenin, acacetin, and isoquercetin, which have anti-obesity, antimicrobial, immune-boosting, antioxidant, anticancer, and anti-inflammatory properties (Shao et al., 2020).

*Lactococcus lactis* is an anaerobic, gram-positive bacterium that can survive at a low pH and reaches the intestine in an active form. It can also modulate immune and inflammatory signaling by enhancing macrophage activity (Song et al., 2017). A recent study showed that *L. lactis* inhibited 3T3-L1 cell differentiation by 67%, decreased the body weight and fat mass of HFD-induced mice, and regulated the expression of fatty acid synthase and PPARγ (Jeong et al., 2023). Although research into adipocyte differentiation via *C. indicum* L. and lactic acid bacteria (LAB) has been conducted, few studies have investigated how increasing the inhibitory effect of fermentation affects adipocyte differentiation using Hh signaling as the main target.

In this study, therefore, we selected the optimal fermentation LAB to enhance the inhibitory effect of *C. indicum* L. on adipocyte differentiation, identified the association between adipocyte differentiation transcription factors and Hh signaling, and elucidated the mechanism underlying the inhibitory effect of the activity of the GLI protein, one of the main targets of Hh signaling, on adipocyte differentiation.

## MATERIALS AND METHODS

### Strain determination and enzyme solution preparation

The Korean Collection for Type Cultures (KCTC) of five LAB strains (*Lactobacillus rhamnosus* KCTC 3237, *Lactococcus lactis* KCTC 3115, *Lactobacillus paracasei* KCTC 3074, *Lactobacillus casei* KCTC 3109, and *Lactobacillus plantarum* KCTC 3107) were used in the experiments. For cellulose degradation assessment, the procured LAB were inoculated into carboxymethyl cellulose (CMC) medium and cultivated for 24 h at 30°C to determine the growth (measured at $OD_{600}$) and the change in pH. The enzyme solution was prepared by inoculating the strain at a concentration of $1\times10^9$ CFU/mL into MRS broth (10% v/v) and incubating the culture at 30°C for 10 h. After centrifugation at 3,000 *g*, the supernatant was used as the enzyme solution.

### Measuring the carboxymethyl cellulose (CMC) resolution

For the degradation measurements, the levels of carboxymethyl cellulase (CMCase) and filter paper hydrolase (FPase) were measured. The CMCase measurements were performed by mixing 2% CMC with the enzyme solution in a 1:9 (v/v) ratio, followed by incubation at 30°C for 4 h. The quantity of sugar produced during the reaction was measured using the 3,5-dinitrosalicylic acid (DNS) method (Miller, 1959). In brief, the sample was mixed with DNS solution in a 1:4 (v/v) ratio and then heated for 5 min in a water bath at 90°C. After cooling, the absorbance was measured at 540 nm. The enzyme activity was expressed as the amount of glucose produced by 1 mg of sample in 1 min, correlating to 1 unit. The FPase measurement was performed by mixing the enzyme solution with filter paper (No. 1, Whatman, Inc.) in a 1:5 (v/w) ratio. Then the same steps described above for CMCase measurement were followed.

### Identification and fermentation of bacterial growth according to the quantity of added *C. indicum* L. extract

Korean *C. indicum* L. was purchased from Dongyang

Oriental Herbal Medicine, and only the petals were used in this experiment. The extraction and fermented product preparation processes were conducted by applying the methods described by Choi et al. (2020). To determine the presence or absence of fermentation depending on the concentration of *C. indicum* L., different proportions of *C. indicum* L. (5%, 10%, 20%, and 40%; v/w) were added to 500 mL of 70% ethyl alcohol and the extraction was allowed to proceed for 48 h. The extract (CI) was filtered through a circular 300-mm filter paper (Advantech) and concentrated to a volume of 10% after decompression at 45°C for 30 min.

For the bacteria, the five LAB strains were inoculated at $OD_{700}$ into MRS medium and then diluted with a 1% ratio (v/v) of the concentrated CI for fermentation. After 24 h of fermentation at 30°C, bacterial growth was checked by measuring the absorbance at $OD_{600}$ and by measuring the pH value of the media.

**Flavonoid and polyphenol content measurement**

The flavonoid and polyphenol contents were measured by following the procedures described in previous studies (Cornard and Merlin, 2002; Dewanto et al., 2002) with some modifications. The flavonoid content was measured by reacting 1 mL of each sample with 1 mL of 10% $AICI_3$. Then, 200 μL of this solution was transferred to a 96-well plate (SPL Life Science), and the absorbance was measured at 405 nm to assess the conversion to quercetin (Sigma-Aldrich). The polyphenol content was determined by adding 1 mL of Folin-Ciocalteu reagent (Junsei Chemical Co., Ltd.) to 1 mL of each sample, stabilizing for 5 min, and then adding 1 mL of 10% $NA_2CO_3$ to induce the reaction for 15 min. The reaction-induced sample was measured at 725 nm to assess the conversion to gallic acid (Sigma-Aldrich).

**DPPH and ABTS radical scavenging activities assessment**

For the measurement of antioxidant capability, the 2,2-diphenyl-1-picrylhydrazyl (DPPH) and 2,2'-azino-bis(3-ethylbenzothiazoline-6-sulfonate) (ABTS) radical scavenging activities were measured according to previous studies (Blois, 1958; Re et al., 1999) with some modifications. The DPPH radical scavenging capacity was determined by dissolving a solution of DPPH (Sigma-Aldrich) in 70% ethanol and adjusting its density to 0.8 at 540 nm. The scavenging capacity (%) was calculated by adding 1 mL of DPPH solution to 1 mL of each sample, reacting for 30 min, and measuring the absorbance at 540 nm. The ABTS radical scavenging capacity was determined by making a solution of ABTS (Sigma-Aldrich), with DW as the solvent, to a concentration of 7.4 mM, adding ammonium persulfate (2.45 mM), inducing 8 h of color development, and adjusting to 0.8 at 740 nm. After adding 1 mL of ABTS solution to 1 mL of each sample, the reaction was initiated for 30 min. Then, the absorbance was measured at 740 nm, and the scavenging capacity (%) was calculated.

**Cell culture and MTT assay**

Cytotoxicity was assessed using 3T3-L1 cells (Korean Cell Line Bank) to set the experimental concentration. Cells were cultured in 96-well plates at a density of $1\times10^4$ cells/well in Dulbecco's modified Eagle's medium (DMEM, HyClone™) supplemented with 10% fetal bovine serum (FBS, Thermo Fisher Scientific) and 1% penicillin-streptomycin (Capricorn Scientific GmbH) in an incubator (WS-180CA, World Science) at 37°C and 5% $CO_2$. The 3-(4,5-dimethylthiazol-2-yl)-2,5-diphenyltetrazolium bromide (MTT) assay was performed by diluting the CI and all fermentation products to 0.125, 0.25, 0.5, and 1 mg/mL in DMEM broth and removing the suspended solids using a 0.22-μm syringe filter (Whatman, Inc.). 3T3-L1 cells were cultivated in 96-well plates at a density of $5\times10^3$ cells/well for 24 h and then incubated for 48 h in DMEM while the samples were treated with different concentrations of CI (0.125, 0.25, 0.5, and 1 mg/mL). After removing the supernatant from each well, 100 μL of MTT (Sigma-Aldrich) solution at a concentration of 5 mg/mL was added, and crystallization was allowed to proceed for 3 h. After crystallization, the crystals were redissolved in dimethyl sulfoxide (DMSO) and the cell viability was measured using an enzyme-linked immunosorbent assay (ELISA) reader at 540 nm (Microplate Reader, Synergy HT, BioTek Instruments).

**Cell differentiation and oil red O staining**

The 3T3-L1 cell lines were cultured in DMEM medium containing 10% FBS and 1% penicillin-streptomycin at a density of $3.5\times10^5$ cells/well in 96-well plates for 24 h to achieve 100% confluence. The medium was then exchanged with 10% FBS differentiation medium containing 10 μg/mL insulin, 0.1 mM dexamethasone, and 0.5 mM 3-isobutyl-1-methylxanthin (IBMX, Sigma-Aldrich) to induce differentiation for 72 h. After 72 h, the medium was exchanged with 10% FBS medium with 10 μg/mL insulin, and the CI and each ferment was treated at 1 mg/mL. Every 72 h, the medium was replaced with fresh insulin-containing medium, and the cultures were maintained for 9 days. Cultured cells were washed with phosphate-buffered saline (PBS, Capricorn Scientific GmbH) and fixed with 10% formaldehyde for 2 h at room temperature. After the formaldehyde was removed, 60% isopropanol (Sigma-Aldrich) was added and removed, and the cells were dried. Oil red O (ORO, Sigma-Aldrich) solution was then added, and the cells were observed after 1 h of incubation. The experiment was terminated by the addition of 60% isopropanol. ORO staining was observed at 510 nm on a microplate reader (Synergy HT,

BioTek Instruments).

### Total protein expression analysis

The 3T3-L1 cell line was seeded at a density of $4.5\times10^5$ cells/well in 60-mm cell culture dishes (SPL Life Science) for 12 h, treated with CI and each ferment at 1 mg/mL for 24 h, and collected after 24 h of incubation. The collected cells were washed twice with PBS and lysed using phosphatase inhibitor cocktail (ATTO Corporation) and protease inhibitor cocktail (ATTO Corporation) in radio-immunoprecipitation assay lysis buffer (ATTO Corporation) and cold-treated for 1 h. After lysis, the cells were centrifuged at 15,814 *g* for 10 min, after which the supernatant was collected and the protein expressions of GLI1, GLI2, GLI3, SMO, PTCH1, PPARγ, C/EBPα, phosphorylated AMP-activated protein kinase (pAMPK, MyBioSource) were measured at 450 nm on an ELISA reader (Microplate Reader, Synergy HT, BioTek Instruments).

### Ultra-high performance liquid chromatography-tandem mass spectrometry (UHPLC-MS/MS) analysis

UHPLC-MS/MS was used to analyze the CI and the active ingredients in the ferments. UHPLC was performed using a Vanquish Flex UHPLC (Thermo Fisher Scientific) with an Agilent C18 column (5 μm, 4.6×250 mm). MS/MS was performed using the TSQ Altis system (Thermo Fisher Scientific). The mobile phases were Milli-Q grade water (Millipore) and acetonitrile (ACN) HPLC grade (J. T. Baker); acetic acid (Merck), 1% acetic acid aqueous solution (solvent A), and 1% acetic acid ACN solution (solvent B) were used as solvents. UHPLC analysis was performed at a column temperature of 40°C. A 10 μL sample was injected at a flow rate of 0.3 mL/min and separated under gradient conditions (30 min with solvent B 5%−95%). MS/MS analysis was performed using negative ion mode electrospray ionization, a nebulizer, high purity nitrogen as an auxiliary gas, and argon as a collision gas.

### Statistical analysis

All experiments were repeated at least three times, and the results were calculated as the mean±standard deviation. Statistical significance tests were performed by one-way analysis of variance in Graph Pad Prism 5 software (Graph Pad Software, Inc.), and post-hoc tests were performed using Turkey's test, where a *P*-value of $<0.05$ was considered statistically significant.

## RESULTS AND DISCUSSION

### Cellulose degradation by LAB and their growth in response to *C. indicum* L. addition

Viscozymes and tannases are groups of enzymes involved in cellulose degradation, and include cellulases, arabinases, β-glucanases, hemicellulases, and xylanases (Juhnevica-Radenkova et al., 2021). Notably, treatment of CI with viscozyme and tannase reduces PPARγ and C/EBPα expression (Lee et al., 2019). This indicates that different strains may exhibit different cellulose degradation abilities. Therefore, cellulose resolution can be used to screen for LABs that enhance the inhibitory effect of *C. indicum* L. on adipocyte differentiation via fermentation.

Each strain was fermented in CMC medium for 24 h. To enhance the readability of the data, LABs were labeled using LAB KCTC numbers. Plant-derived strain 3107, with an $OD_{600}$ value of 0.31±0.01, a pH value of 4.61±0.03, a CMCase activity of 0.69±0.03 unit/mL, and an FPase activity of 0.66±0.03 unit/mL, showed a significantly higher cellulose degradation capacity than any of the other strains. All other strains had $OD_{600}$ values ranging from 0.07 to 0.13, pH values ranging from 5.8 to 6.8 (Fig. 1A), CMCase activity ranging from 0.02 to 0.17 unit/mL, and FPase activity ranging from 0.003 to 0.13 unit/mL. Strains 3074 and 3237 showed poorer cellulose degradation compared to the other strains (Fig. 1B).

To determine *C. indicum* L. resistance in LAB, the $OD_{600}$ value and pH as a function of the amount of *C. indicum* L. added were identified. For strains 3074 and 3237, compared to CI, the LAB growth decreased with the addition of *C. indicum* L. In contrast, strains 3109 and 3115 exhibited growth up to a 20% concentration but decreased at a 40% concentration (Fig. 1C). Regarding pH values, only strain 3107 maintained a pH around 3 at all concentrations, while the other strains showed little change after the 20% concentration (Fig. 1D). The antimicrobial effects of *C. indicum* L. involved hexokinase and pyruvate kinase, and it can be speculated that the effectiveness of *C. indicum* L. increased as the amount of added *C. indicum* L. increased. This seems to apply equally to LAB (Lin et al., 2019). Based on this data, we decided to use 20% *C. indicum* L. in the subsequent experiments.

### Fermentation process of *C. indicum* L. extract

The CI/LAB fermentations were conducted as follows. The fermentations were labeled according to the LAB used such that the fermentations involving *L. rhamnosus* KCTC 3237, *L. lactis* KCTC 3115, *L. paracasei* KCTC 3074, *L. casei* KCTC 3109, and *L. plantarum* KCTC 3107 were labeled LRF37, LLF15, LPF74, LCF09, and LPF07, respectively. To verify the fermentation process of each LAB, fermentation was conducted for 48 h with 20% *C. indicum* L., and the growth rate and pH were measured. Under typical medium conditions, *Lactobacillus* is known to terminate proliferation within 24 h, with culture ter-

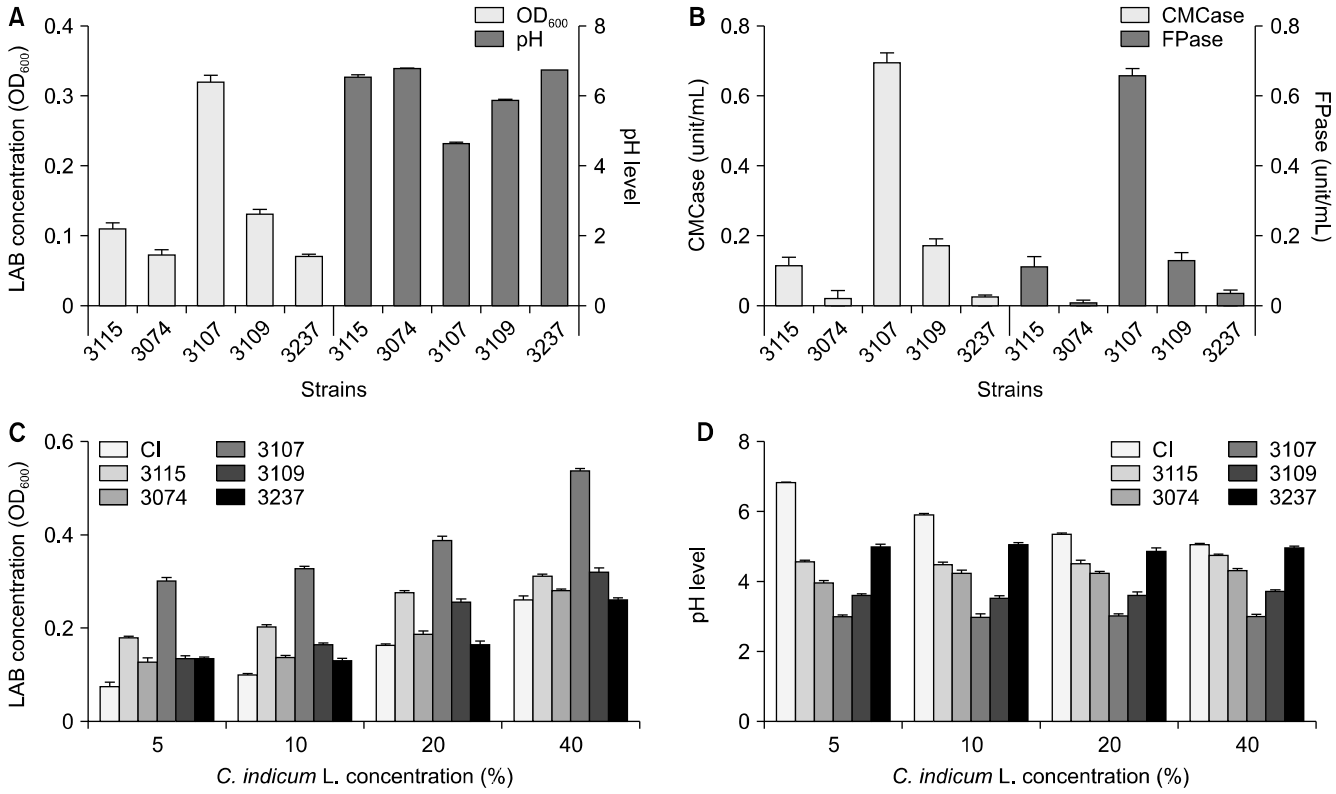


**Fig. 1.** Enzymatic characterization of lactic acid bacteria (LAB) and identification of LAB resistance in *Chrysanthemum indicum* L. After incubation in carboxymethyl cellulose (CMC) medium at 30°C for 24 h to determine LAB growth and pH reduction (A), the carboxymethyl cellulase (CMCase) and filter paper hydrolase (FPase) activity (B) were measured, and the growth rate (C) and pH were determined (D) in response to the addition of *C. indicum* L. These parameters were measured in the *C. indicum* L. extract (CI), and in the fermentations using *Lactococcus lactis* KCTC 3115 (3115), *Lactobacillus paracasei* KCTC 3074 (3074), *Lactobacillus casei* KCTC 3109 (3109), *Lactobacillus plantarum* KCTC 3107 (3107), and *Lactobacillus rhamnosus* KCTC 3237 (3237). Values are presented as the mean±SD (n=3).

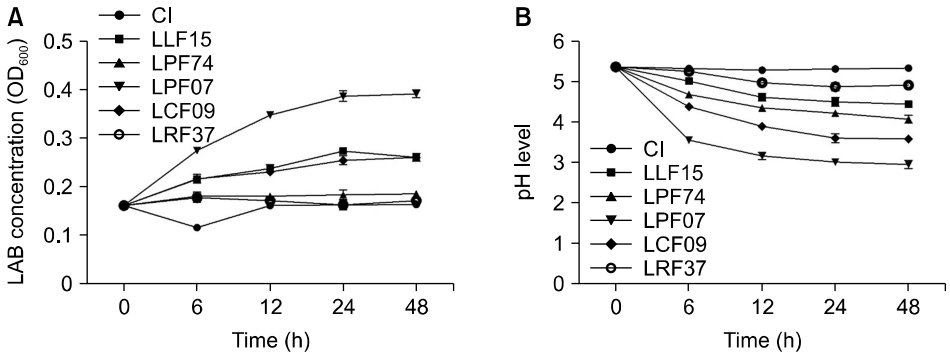


**Fig. 2.** Changes during 48-h fermentation after the addition of 20% *C. indicum* L. Lactic acid bacteria (LAB) concentration (A) and pH changes (B) during fermentation. Values are presented as the mean±SD (n=3). CI, *C. indicum* L. extract; LLF15, CI fermented with *L. lactis* KCTC 3115; LPF74, CI fermented with *L. paracasei* KCTC 3074; LPF07, CI fermented with *L. plantarum* KCTC 3107; LCF09, CI fermented with *L. casei* KCTC 3109; LRF37, CI fermented with *L. rhamnosus* KCTC 3237.

mination occurring around pH 3–4. *Lactococcus* is also known to experience a proliferation shutdown at 24 h, terminating at around pH 4–5, with low lactic acid production compared to other strains (Rallu et al., 1996; Goderska et al., 2002; Souza et al., 2017). In this study, it was found that LPF07 growth reduced at a pH of around 3, whereas LLF15 showed growth arrest around pH 4.5 (Fig. 2B). The growth of LPF07, LLF15, and LCF09 was confirmed in this order, whereas LPF74 and LRF37 were not significantly different from CI (Fig. 2A).

### Flavonoid and polyphenol contents and antioxidant power

Oxidative stress has been linked to many diseases, including obesity and cardiovascular conditions. Oxidative stress, which is increased by the production of reactive oxygen species (ROS), is known to accelerate obesity by increasing the differentiation rate of adipose precursor cells and the size of adipocytes. Previous studies have reported that increased antioxidant capacity can have positive effects on obesity-related conditions due to the in-

hibition of ROS production (Zielinska-Blizniewska et al., 2019; Choi et al., 2022).

To determine the antioxidant capacity of the CI and fermentation products, the flavonoid and polyphenol contents and the DPPH and ABTS radical scavenging capacities were determined. The CI had a flavonoid content of 0.153±0.001 mg/mL, whereas LLF15, LPF74, LPF07, LCF09, and LRF37 showed flavonoid contents of 0.129±0.001 mg/mL, 0.135±0.001 mg/mL, 0.116±0.001 mg/mL, 0.143±0.001 mg/mL, and 0.135±0.001 mg/mL, respectively, indicating a significant ($P$<0.001) decrease in flavonoid content in the fermentation groups compared to CI ($P$<0.001) (Fig. 3A). The CI showed a polyphenol content of 0.482±0.009 mg/mL, while LLF15, LPF74, LPF07, LCF09, and LRF37 showed polyphenol contents of 0.467±0.006 mg/mL, 0.490±0.009 mg/mL, 0.440±0.009 mg/mL, 0.491±0.012 mg/mL, and 0.511±0.005 mg/mL, respectively. The polyphenol content in the LPF07 fermentation was significantly ($P$<0.001) lower and that in the LRF37 fermentation (Fig. 3B) significantly ($P$<0.05) higher than that in the CI. LLF15 showed a lower polyphenol content than the CI, and LPF74 and LCF09 showed higher polyphenol contents than the CI; however, these differences were not statistically significant. The CI showed a DPPH radical scavenging activity of 43.53%±0.45%. The DPPH radical scavenging activity was 52.46%±1.71% for LLF15, 55.52%±2.64% for LPF74, 49.24%±2.57% for LPF07, 55.40%±2.64% for LCF09, and 54.00%±1.57% for LRF37 (Fig. 3C). The DPPH radical scavenging activity was significantly higher ($P$<0.01, $P$<0.001) in the fermentation group compared to the CI. The ABTS radical clearance was 49.75%±2.70% for the CI, 59.34%±3.33% for LLF15, 61.31%±2.41% for LPF74, 50.16%±1.73% for LPF07, 59.43%±3.64% for LCF09, and 56.89%±5.71% for LRF37 (Fig. 3D). All fermentations exhibited higher ABTS radical clearance than the CI, and all but LPF07 were significant ($P$<0.01, $P$<0.001). In this study, the flavonoid content decreased in the fermented group compared to the CI, whereas the polyphenol content showed little change and even decreased in the fermented group. The DPPH and ABTS radical scavenging capacities were found to increase in the fermentation group.

In general, polyphenols and flavonoids are considered benchmarks for evaluating antioxidant capacity, and their contents are increased by enzymes that are produced during fermentation to break down cellulose and other factors. However, prolonged fermentation is known to decrease the polyphenol and flavonoid contents due to ROS produced during microbial metabolism and enzymes that degrade polyphenols and flavonoids (Adetuyi and Ibrahim, 2014). In this study, we found that the

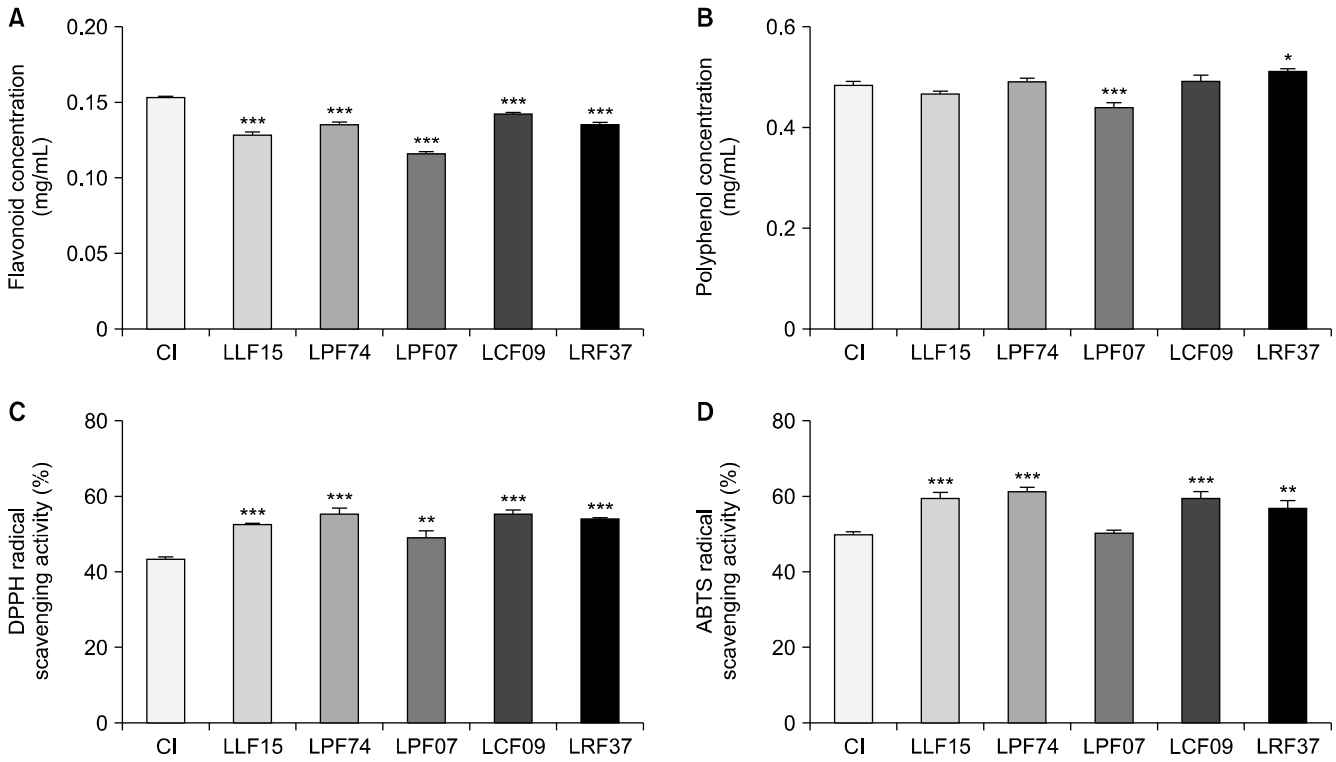


**Fig. 3.** Comparative antioxidant capacity. Total flavonoid content (A), total polyphenol content (B), 2,2-diphenyl-1-picrylhydrazyl (DPPH) (C) and 2,2′-azino-bis(3-ethylbenzothiazoline-6-sulfonate) (ABTS) (D) radical scavenging capacity of *C. indicum* L. extract (CI) and ferments as a measure of the antioxidant capacity. Values are presented as the mean±SD (n=3). *$P$<0.05, **$P$<0.01, and ***$P$<0.001 versus CI group. LLF15, CI fermented with *L. lactis* KCTC 3115; LPF74, CI fermented with *L. paracasei* KCTC 3074; LPF07, CI fermented with *L. plantarum* KCTC 3107; LCF09, CI fermented with *L. casei* KCTC 3109; LRF37, CI fermented with *L. rhamnosus* KCTC 3237.

contents of flavonoids and polyphenols decreased, whereas the antioxidant capacity increased. This may have been due to the measurement methods or the fermentation process. When determining flavonoid content via the color difference caused by aluminum binding to flavonoids, the absorbances of different types of flavonoids, such as quercetin, rutin, and catechin, exhibit differences (Shraim et al., 2021). This difference in absorbance due to aluminum binding is likely caused by the creation of a component with a lower charge but a higher antioxidant capacity. In the case of polyphenols, this includes various components, with a decrease in polyphenols correlating poorly with a decrease in antioxidant capacity (Pompeu et al., 2021). A recent study assessed the components in green tea after fermentation and found that while the polyphenol content decreased, the antioxidant capacity was maintained or increased (Xu et al., 2022). Another possibility for this phenomenon is that the increased DPPH and ABTS radical scavenging capacities may have been caused by the enzymatic degradation of some polyphenols and proteins from their macromolecular form into small molecules (Chen et al., 2013).

### 3T3-L1 cell viability as a function of CI and each fermentation treatment concentration

To determine the cytotoxicity of CI and each fermentation treatment concentration, cell viability was measured using 3T3-L1 cells. CI was added to 3T3-L1 cells at concentrations of 0.125, 0.25, 0.5, and 1 mg/mL. The cell viability rates were 101.4%±3.3%, 94.5%±5.1%, 91.0%±2.6%, and 82.8%±2.5%, respectively for the 0.125, 0.25, 0.5, and 1 mg/mL concentrations of CI, indicating minimal cytotoxicity even at the highest concentration of 1 mg/mL. The cell viability rate decreased with the treatment concentration. In LRF37, the cell viability rates were 94.7%±3.6%, 90.5%±2.3%, 92.1%±3.2%, and 89.7%±3.7% for the 0.125, 0.25, 0.5, and 1 mg/mL treatments, respectively, with higher cell viability rates observed compared to the CI at concentrations above 0.5 mg/mL. LPF74 showed cell viability rates of 102.9%±0.8%, 96.7%±2.0%, 92.1%±4.9%, and 81.6%±5.2% for the 0.125, 0.25, 0.5, and 1 mg/mL treatments, respectively, whereas LPF07 showed rates of 115.8%±3.0%, 107.1%±4.3%, 89.1%±4.4%, and 82.1%±4.4%, respectively. LCF09 showed cell viability rates of 103.6%±4.7%, 102.1%±4.2%, 83.5%±4.9%, and 74.9%±3.4%, respectively, and LLF15 showed rates of 98.3%±3.7%, 100.3%±2.6%, 93.8%±2.1%, and 88.6%±1.6%, respectively (Fig. 4). Each fermentation group showed almost the same cell viability rates as the CI, and some treatment concentrations showed higher cell viability rates than the CI.

LAB are thought to protect cells from the oxidative stress caused by toxicity and inhibit cell death. LPF07 showed a higher cell viability rate than the CI. *L. plantarum*, a plant-derived LAB, is known to protect IPEC-J2 cells from $H_2O_2$-induced cytotoxicity and mitigate cell death (Wang et al., 2021a). Each fermentation, with the exception of LCF09, showed cell viability rates of greater than 80% at a concentration of 1 mg/mL of treatment; therefore, the subsequent experiments were conducted using a treatment concentration of 1 mg/mL.

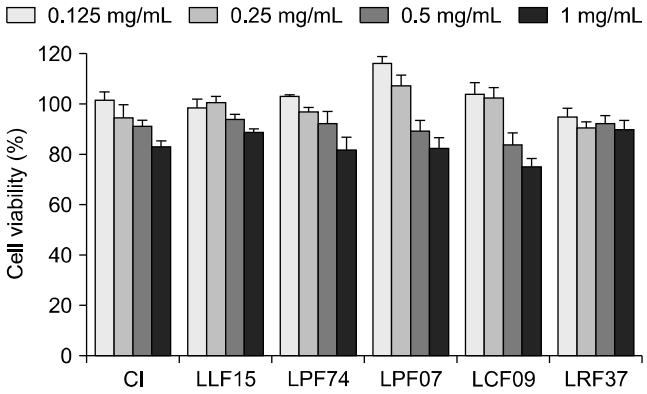


**Fig. 4.** Viability of 3T3-L1 cells treated with *C. indicum* L. extract (CI) and ferments. Concentration-dependent cytotoxicity was measured and expressed as cell viability. Values represent the mean±SD (n=3). LLF15, CI fermented with *L. lactis* KCTC 3115; LPF74, CI fermented with *L. paracasei* KCTC 3074; LPF07, CI fermented with *L. plantarum* KCTC 3107; LCF09, CI fermented with *L. casei* KCTC 3109; LRF37, CI fermented with *L. rhamnosus* KCTC 3237.

### Differentiation based on adipocyte transcription factors in CI and fermentation products

During the differentiation of adipocyte progenitors into adipocytes, two transcription factors, C/EBPβ and C/EBPδ, influence early differentiation, and two complementary transcription factors, PPARγ and C/EBPα, drive late differentiation. Stimulation with IBMX, DMSO, insulin, etc., induces differentiation results in the expression of C/EBPβ and C/EBPδ and induces the expression of terminal makers such as adiponectin and the glucose transporter (Cao et al., 1991; Rosen et al., 2002; Rosen and MacDougald, 2006; Zebisch et al., 2012). As a central regulator of cellular metabolism, AMP-activated protein kinase (AMPK) mediates the phosphorylation of target substrates and is essential for the regulation and maintenance of energy homeostasis. AMPK phosphorylation promotes biosynthetic pathways and regulates fatty acid production to increase energy expenditure. It is therefore considered a key target for the prevention and treatment of obesity (Choi et al., 2024; Wang et al., 2021b).

ORO staining was used to confirm the differentiation of adipocytes. Compared to the differentiation-induced 3T3-L1 cells treated with DMSO (MDID) group, adipocyte differentiation was significantly inhibited (to 75.8%±3.7%; $P<0.001$) by the addition of CI. Adipocyte differentiation inhibition was measured at 66.3%±2.9% for

LPF74, 64.0%±4.1% for LPF07, 75.6%±5.6% for LCF09, 59.2%±3.7% for LLF15, and 64.5%±2.2% for LRF37 (Fig. 5B). Microscopic observation confirmed that the inhibition of differentiation was more effective in the LLF15 group than in the other fermentation groups (Fig. 5A). As measured using ELISA to investigate protein expression, each fermentation product, including CI, exhibited suppressed expression of all adipocyte transcription factors compared with that of the MDID group. The protein expression of PPARγ was 4.155±0.018 for CI, 3.158±0.014 for LPF74, 3.299±0.020 for LPF07, 4.127±0.025 for LCF09, 2.832±0.018 for LLF15, and 3.493±0.028 for LRF37, confirming that the CI and each fermentation product conferred significant ($P$<0.001) inhibition compared to the MDID group (Fig. 5C). The expressions of C/EBPα and pAMPK were significantly ($P$<0.001) inhibited by CI and all fermentation groups, with LLF15 conferring the lowest expressions (1.003±0.013 and 7.533±0.133 for C/EBPα and pAMPK, respectively) (Fig. 5D and 5E). The results showed that CI and each fermentation product inhibited the differentiation of adipocytes through relevant transcription factors. However, in some fermentation groups, such as the LLF15 group, it was observed that adipocyte differentiation was excessively inhibited, and the number of already differentiated adipocytes was reduced (Fig. 5A and 5B). This suggests that adipocyte differentiation is inhibited by signals independent of adipocyte differentiation signals. Hh signaling in 3T3-L1 cells is known to regulate the upstream signaling of PPARγ to induce adipogenesis (Suh et al., 2006). Therefore, we aimed to determine the relationship between Hh signaling, a type of adipocyte progenitor cell signaling, and adipocyte signaling.

**CI and Hh signaling in the fermentation products**

Ligands involved in Hh signaling bind to PTCHs and activate SMO. Among the two PTCH proteins, PTCH1 is directly involved in Hh signaling to activate SMO. Activated SMO translocates GLI family proteins (GLI1, GLI2, and GLI3), which are cleaved from the SUFU, into the nucleus of the cell to promote the transcription of target genes (Cousin et al., 2007; Hu et al., 2015; Pak and Segal, 2016). GLI1 and GLI2 are primarily transcriptional activators, whereas GLI3 is involved in transcriptional repression (Jia et al., 2003). Several transcription factors involved in the Hh signaling pathway (PTCH1, SMO, GLI1, GLI2, and GLI3) maintain Hh signaling activity, among which GLI1 is a highly reliable target gene of Hh signaling (Fontaine et al., 2008). Several transcription factors involved in Hh signaling have been implicated in adipocyte differentiation, and in particular, GLI1 overexpression has been demonstrated to inhibit fat accumulation in adipocytes by reducing the control of PPARγ, a transcription factor for adipocyte differentiation, and the expression of C/EBPα, which drives late adipocyte differentiation, to reduce the development of obesity and diabetes (Darlington et al., 1998; Fan et al., 2018; Zhou et al., 2022; Zou et al., 2022).

PTCH1 protein expression was significantly ($P$<0.001) lower in the CI and all fermentation groups compared to the MDID group, with LLF15 and LRF37 exhibiting lower expression than other fermentation groups, with values of 18.621±0.618 and 20.630±0.548, respectively (Fig. 6A). However, SMO protein expression was significantly higher ($P$<0.001) in the MDID group than in the CI and each fermentation group, with LLF15 showing high SMO expression compared to other groups (5.158±0.063) (Fig. 6B). GLI1 protein expression was significantly higher in the LLF15 and LRF37 groups compared to the other fermentation groups ($P$<0.001), with values of 2.353±0.146 and 1.842±0.144, respectively (Fig. 6C). The protein expression of GLI2 was higher in LCF09 only, at 1.770±0.343, but this difference was not significant (Fig. 6D). Conversely, GLI3 protein expression was significantly higher ($P$<0.001) in LLF15, LCF09, and LRF37, at 2.436±0.050, 2.581±0.068, and 2.342±0.087, respectively (Fig. 6E).

SMO activity was confirmed in all fermentations, including CI, due to the inhibition of PTCH1. GLI1 and GLI3 were active in LLF15 and LRF37, and GLI2 and GLI3 were active in LCF09. The results (Fig. 6) suggested that GLI1 activity inhibited adipocyte differentiation in LLF15 and LRF37. Increased GLI1 protein expression inhibits adipocyte differentiation by controlling the expression of C/EBPα and PPARγ and can reduce body weight gain by affecting visceral white adipose tissue in HFD-induced animals (Qiu et al., 2021; Kim et al., 2024). Among the five LAB that had high antioxidant activity and inhibited the differentiation of 3T3-L1 cells into adipocytes in a concentration-dependent manner, the strains that affected Hh signaling were *L. lactis* KCTC 3115 and *L. rhamnosus* KCTC 3237. These two strains can be considered optimal strains that can inhibit the differentiation of adipocytes by regulating Hh signaling by fermenting *C. indicum* L.

In this study, we aimed to identify substances that effectively regulate GLI1 by analyzing the components of LLF15 and identifying which components possess the highest GLI1 activity and regulate C/EBPα and PPARγ expression by inhibiting 3T3-L1 cell differentiation.

**Composition differences between CI and LLF15**

Each component of CI and LLF15 was analyzed qualitatively via UHPLC-MS/MS. In CI, *p*-coumaric acid (retention time, RT: 9.84) was detected (Fig. 7A), which was not detected in LLF15, while rhoifolin (RT: 11.72), quercetin (RT: 14.93), daidzein (RT: 14.01), and genistein

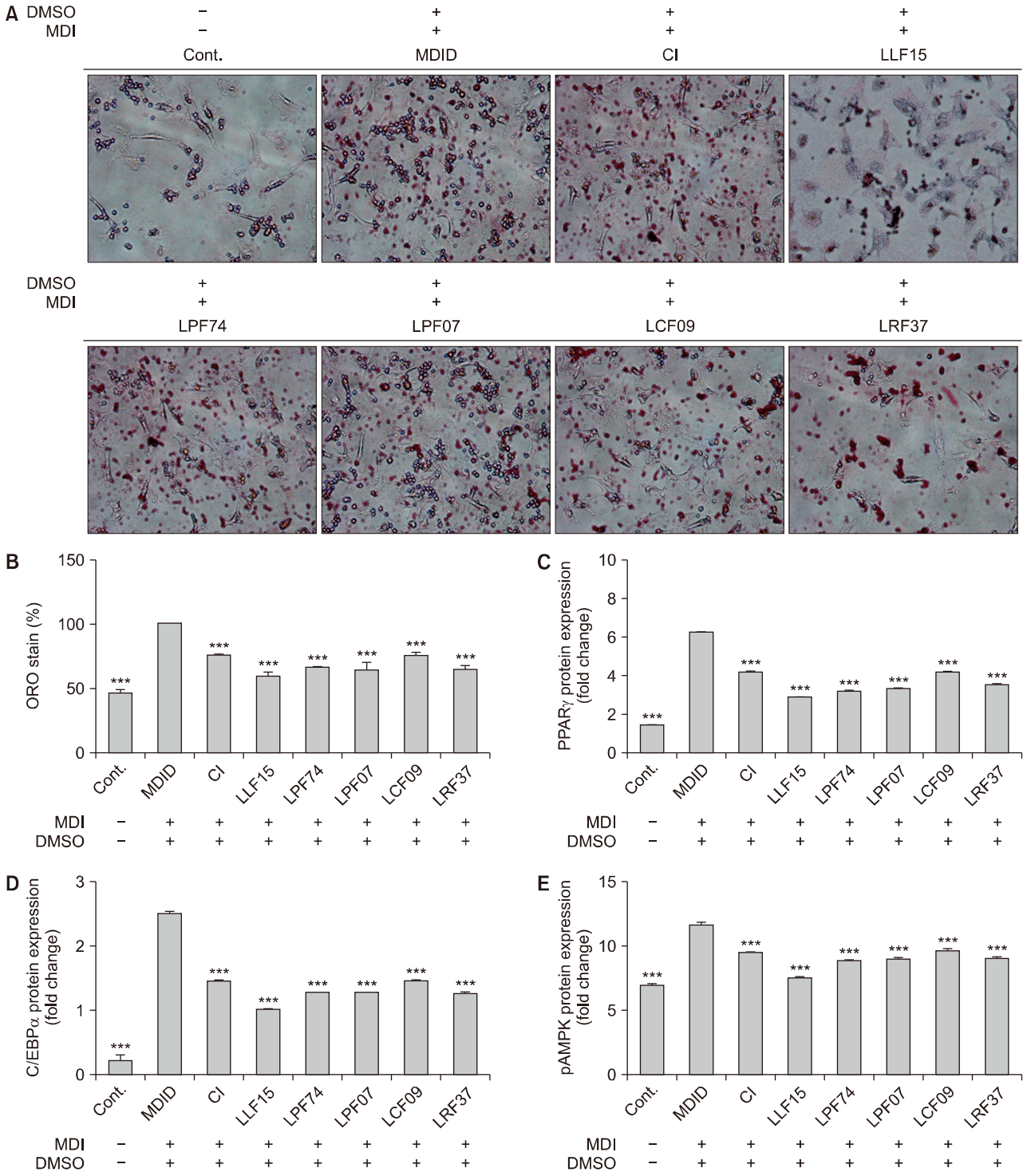


**Fig. 5.** Identification of adipocyte differentiation using oil red O (ORO) staining and adipogenesis signaling using protein expression. Adipocyte morphology was assessed in 3T3-L1 cells (A) and plotted (B). Peroxisome proliferator-activated receptor-γ (PPARγ) (C), CCAAT/enhancer binding protein-α (C/EBPα) (D), and phosphorylated AMP-activated protein kinase (pAMPK) (E) protein expression was measured using enzyme-linked immunosorbent assay (ELISA). Comparison of undifferentiated 3T3-L1 cells (Cont.), differentiation-induced 3T3-L1 cells (MDI), differentiation-induced 3T3-L1 cells treated with DMSO (MDID), and their respective controls. Values represent the mean±SD (n=3). ***$P$<0.001 versus MDID group. DMSO, dimethyl sulfoxide; CI, *C. indicum* L. extract; LLF15, CI fermented with *L. lactis* KCTC 3115; LPF74, CI fermented with *L. paracasei* KCTC 3074; LPF07, CI fermented with *L. plantarum* KCTC 3107; LCF09, CI fermented with *L. casei* KCTC 3109; LRF37, CI fermented with *L. rhamnosus* KCTC 3237.

(RT: 16.53) were additionally detected in LLF15 (Fig. 7B). Among these components, luteolin and quercetin, which are known to be typical antioxidants and phenolic substances that inhibit obesity, were quantitatively analyzed. The results showed an 11.8% increase in luteolin and a 400% increase in quercetin in the LLF15 fermentation

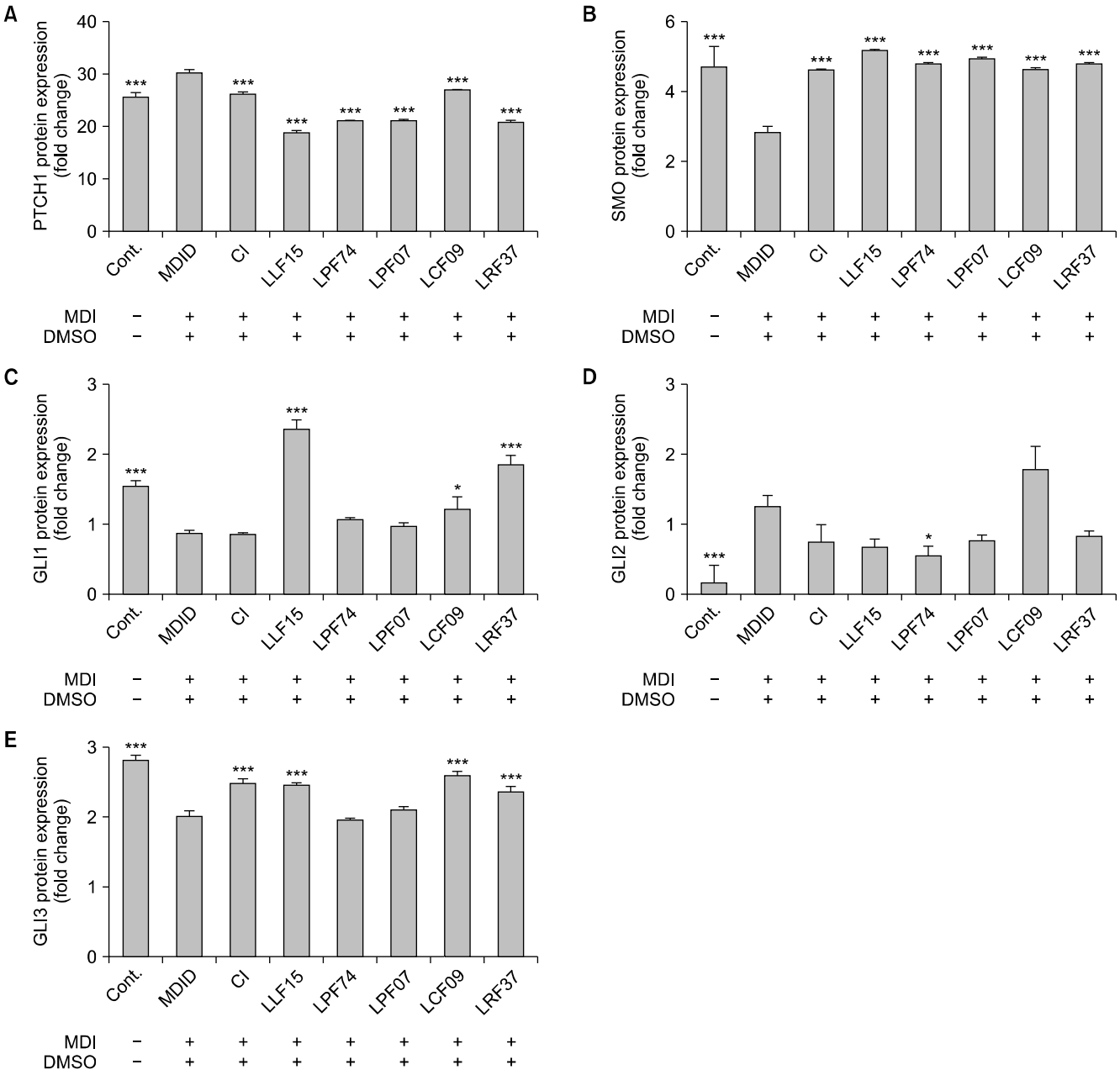


**Fig. 6.** Protein expression of hedgehog signaling in differentiated 3T3-L1 cells. Patched 1 (PTCH1) (A), smoothened (SMO) (B), and glioma-associated oncogene 1, 2, 3 (GLI1, 2, 3) (C, D, E) protein expression measured using enzyme-linked immunosorbent assay (ELISA). Values represent the mean±SD (n=3). $^{*}P<0.05$ and $^{***}P<0.001$ versus differentiation-induced 3T3-L1 cells treated with DMSO (MDID) group. Cont., undifferentiated 3T3-L1 cells; CI, *C. indicum* L. extract; LLF15, CI fermented with *L. lactis* KCTC 3115; LPF74, CI fermented with *L. paracasei* KCTC 3074; LPF07, CI fermented with *L. plantarum* KCTC 3107; LCF09, CI fermented with *L. casei* KCTC 3109; LRF37, CI fermented with *L. rhamnosus* KCTC 3237; MDI, differentiation-induced 3T3-L1 cells; DMSO, dimethyl sulfoxide.

compared to in the CI. Luteolin and quercetin inhibit the differentiation of adipocytes by controlling the expression of PPARγ and C/EBPα, and luteolin is known to be effective even in small doses (Sakuma et al., 2021).

Some of the phenolic substances present in plants affect Hh signaling (Petricci and Manetti, 2015), and microbial fermentation converts glycosides to nonglycosides and nonglycosides to glycosides through glycosylation, deglycosylation, methylation, glucuronidation, and sulfatase conjugation mechanisms via the activity of enzymes such as β-glucosidase, cellulase, and decarboxylase, which are produced by the strain during fermentation. For example, quercetin-glucoside has been reported to be converted to quercetin through the fermentation of *L. plantarum*, and this mechanism is believed to increase the quantity of certain phenolic substances that undergo the fermentation process (Huynh et al., 2014). It can be inferred that an increase in phenolic substances controls the adipocyte differentiation of 3T3-L1 cells by affecting Hh signaling. However, further research into the con-

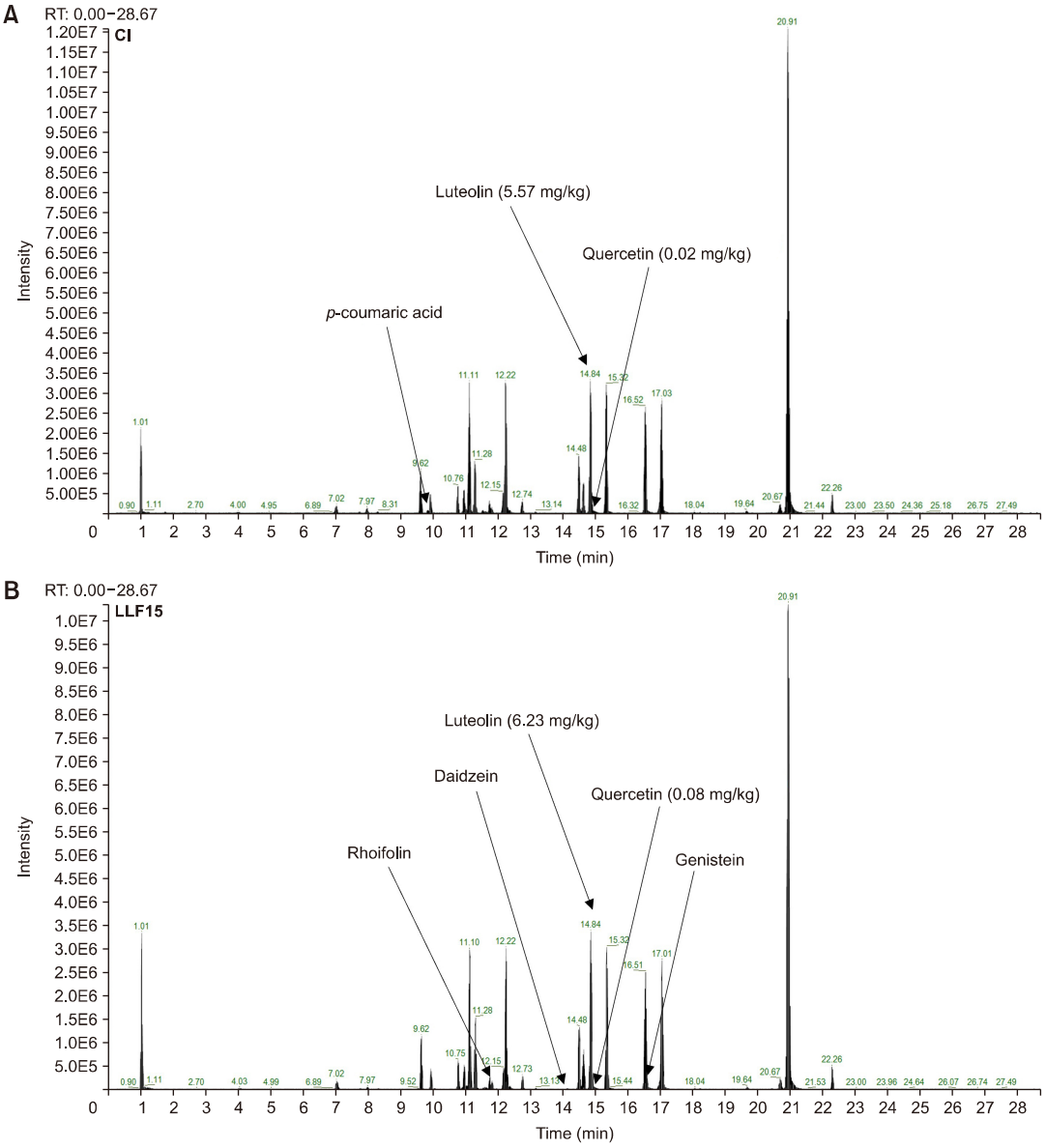


**Fig. 7.** Ultra-high performance liquid chromatography-tandem mass spectrometry analysis of converted chemical derivatives after the fermentation process. Qualitative analysis of chemical derivatives of *C. indicum* L. extract (CI) (A) and CI fermented with *L. lactis* KCTC 3115 (LLF15) (B). RT, retention time.

version process is needed to identify the specific compounds that simultaneously affect adipocyte differentiation and Hh signaling in adipocyte progenitors.

In summary, among the CI and the five fermentation groups, only the LLF15 and LRF37 groups inhibited adipocyte differentiation. Adipocyte differentiation was thought to be inhibited via the suppression of PPARγ, C/EBPα, and pAMPK expression and the regulation of GLI1 in Hh signaling, which are differentiation signals in 3T3-L1 cells. Specifically, the LLF15 group showed the most effective inhibition of adipocyte differentiation, with the highest expression of GLI1 in Hh signaling and lower PPARγ, C/EBPα, and pAMPK expressions than the other comparison groups. In conclusion, *L. lactis* KCTC 3115 enhanced the ability of *C. indicum* L. to regulate Hh signaling and inhibit adipocyte differentiation through fermentation (Fig. 8). LLF15 inhibited adipocyte differentiation by modulating adipocyte differentiation signaling and GLI1 activity of Hh signaling in adipocyte precursor cells. The findings of this study suggest that LLF15 has the potential be developed as a novel obesity medicine that can regulate adipocyte progenitor cell differentiation and inhibit adipocyte differentiation by modulating the activity of GLI1 in Hh signaling.

## FUNDING

This work was supported by the National Research Foundation of Korea (NRF) grant funded by the Korea

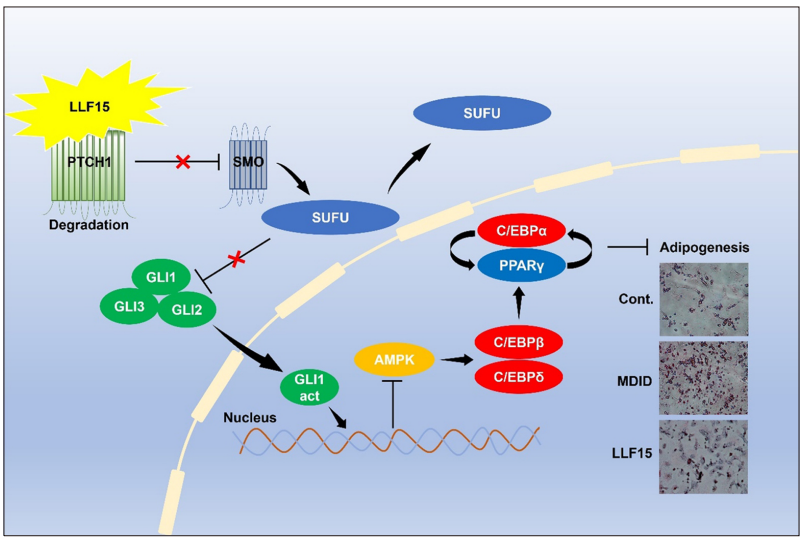


**Fig. 8.** Schematic of the key hedgehog signaling-related transcription factors and how they regulate adipocyte differentiation transcription factors. LLF15, *C. indicum* L. extract fermented with *L. lactis* KCTC 3115; PTCH1, patched 1; SMO, smoothened; SUFU, suppressor of fusion; GLI, glioma-associated oncogene; AMPK, AMP-activated protein kinase; C/EBP, CCAAT/enhancer binding protein; PPARγ, peroxisome proliferator-activated receptor-γ; Cont., undifferentiated 3T3-L1 cells; MDID, differentiation-induced 3T3-L1 cells treated with dimethyl sulfoxide.

government (MSIT) (RS-2022-00166584). This work was supported by Korea Institute of Planning and Evaluation for Technology in Food, Agriculture and Forestry (IPET) through High Value-added Food Technology Development Program, funded by Ministry of Agriculture, Food and Rural Affairs (MAFRA) (119116-01).

## AUTHOR DISCLOSURE STATEMENT

The authors declare no conflict of interest.

## AUTHOR CONTRIBUTIONS

Concept and design: JC. Analysis and interpretation: YJC, JBL, JC. Data collection: YJC, JBL, JC. Writing the article: YJC, JBL, JC. Critical revision of the article: JC. Final approval of the article: all authors. Statistical analysis: MSL, YL. Obtained funding: JC. Overall responsibility: JC.

## REFERENCES

Adetuyi FO, Ibrahim TA. Effect of fermentation time on the phenolic, flavonoid and vitamin C contents and antioxidant activities of okra (*Abelmoschus esculentus*) seeds. Niger Food J. 2014. 32:128-137.

Blois MS. Antioxidant determinations by the use of a stable free radical. Nature. 1958. 181:1199-1200.

Cao Z, Umek RM, McKnight SL. Regulated expression of three C/EBP isoforms during adipose conversion of 3T3-L1 cells. Genes Dev. 1991. 5:1538-1552.

Chen J, Bao C, Kim JT, Cho JS, Qiu S, Lee HJ. Sulforaphene inhibition of adipogenesis via hedgehog signaling in 3T3-L1 adipocytes. J Agric Food Chem. 2018. 66:11926-11934.

Chen J, Liu S, Ye R, Cai G, Ji B, Wu Y. Angiotensin-I converting enzyme (ACE) inhibitory tripeptides from rice protein hydrolysate: Purification and characterization. J Funct Foods. 2013. 5:1684-1692.

Choi DH, Han JH, Hong M, Lee SY, Lee SU, Kwon TH. Antioxidant and lipid-reducing effects of *Rosa rugosa* root extract in 3T3-L1 cell. Food Sci Biotechnol. 2022. 31:121-129.

Choi JY, Lim JS, Sim BR, Yang YH. Inhibitory effect of lactic acid bacteria-fermented *Chrysanthemum indicum* L. on adipocyte differentiation through hedgehog signaling. J Life Sci. 2020. 30:532-541.

Choi YR, Kim YS, Kim MJ. Cinnamyl alcohol attenuates adipogenesis in 3T3-L1 cells by arresting the cell cycle. Int J Mol Sci. 2024. 25:693. https://doi.org/10.3390/ijms25020693

Cornard JP, Merlin JC. Spectroscopic and structural study of complexes of quercetin with Al(III). J Inorg Biochem. 2002. 92:19-27.

Cousin W, Fontaine C, Dani C, Peraldi P. Hedgehog and adipogenesis: Fat and fiction. Biochimie. 2007. 89:1447-1453.

Darlington GJ, Ross SE, MacDougald OA. The role of *C/EBP* genes in adipocyte differentiation. J Biol Chem. 1998. 273: 30057-30060.

Dewanto V, Wu X, Adom KK, Liu RH. Thermal processing enhances the nutritional value of tomatoes by increasing total antioxidant activity. J Agric Food Chem. 2002. 50:3010-3014.

Fan C, Zhang Y, Wang J, Cheng J. Roles of Hedgehog signaling pathway in adipogenic differentiation potential of porcine adipose-derived mesenchymal stem cells. Rev Bras Zootec. 2018. 47:e20170019. https://doi.org/10.1590/rbz4720170019

Fontaine C, Cousin W, Plaisant M, Dani C, Peraldi P. Hedgehog signaling alters adipocyte maturation of human mesenchymal stem cells. Stem Cells. 2008. 26:1037-1046.

Goderska K, Czarnecka M, Czarnecki Z. Survival rate of chosen *Lactobacillus* bacteria type in media of different pH. Electron J Polish Agric Univ. 2002. 5:1-8.

Hu L, Lin X, Lu H, Chen B, Bai Y. An overview of hedgehog signaling in fibrosis. Mol Pharmacol. 2015. 87:174-182.

Huynh NT, Van Camp J, Smagghe G, Raes K. Improved release and metabolism of flavonoids by steered fermentation processes: A review. Int J Mol Sci. 2014. 15:19369-19388.

Jemai R, Drira R, Makni M, Fetoui H, Sakamoto K. Colocynth (*Citrullus colocynthis*) seed extracts attenuate adipogenesis by down-regulating PPARγ/ SREBP-1c and C/EBPα in 3T3-L1 cells. Food Bioscience. 2020. 33:100491. https://doi.org/10.1016/j.fbio.2019.100491

Jeong H, Hwang US, Choi H, Park YS. Assessing the anti-obesity potential of *Lactococcus lactis* subsp. *lactis* CAB701: Modulation of adipocyte differentiation and lipid metabolism in in vitro and in vivo models. Probiotics antimicrob proteins. 2023.

https://doi.org/10.1007/s12602-023-10198-9
Jia J, Tong C, Jiang J. Smoothened transduces Hedgehog signal by physically interacting with Costal2/Fused complex through its C-terminal tail. Genes Dev. 2003. 17:2709-2720.
Juhnevica-Radenkova K, Kviesis J, Moreno DA, Seglina D, Vallejo F, Valdovska A, et al. Highly-efficient release of ferulic acid from agro-industrial by-products via enzymatic hydrolysis with cellulose-degrading enzymes: Part I—the superiority of hydrolytic enzymes versus conventional hydrolysis. Foods. 2021. 10:782. https://doi.org/10.3390/foods10040782
Kim JT, Chen J, Zhou Y, Son MJ, Jeon DH, Kwon JW, et al. Cycloastragenol inhibits adipogenesis and fat accumulation in vitro and in vivo through activating Hedgehog signaling. Food Sci Biotechnol. 2024. 33:711-720.
Lee JH, Moon JM, Kim YH, Lee B, Choi SY, Song BJ, et al. Effect of enzymatic treatment of *Chrysanthemum indicum* Linné extracts on lipid accumulation and adipogenesis in high-fat-diet-induced obese male mice. Nutrients. 2019. 11:269. https://doi.org/10.3390/nu11020269
Lin L, Mao X, Sun Y, Rajivgandhi G, Cui H. Antibacterial properties of nanofibers containing chrysanthemum essential oil and their application as beef packaging. Int J Food Microbiol. 2019. 292:21-30.
Miller GL. Use of dinitrosalicylic acid reagent for determination of reducing sugar. Anal Chem. 1959. 31:426-428.
Moldes M, Boizard M, Liepvre XL, Fève B, Dugail I, Pairault J. Functional antagonism between inhibitor of DNA binding (Id) and adipocyte determination and differentiation factor 1/sterol regulatory element-binding protein-1c (ADD1/SREBP-1c) *trans*-factors for the regulation of fatty acid synthase promoter in adipocytes. Biochem J. 1999. 344:873-880.
Nerurkar PV, Lee YK, Nerurkar VR. *Momordica charantia* (bitter melon) inhibits primary human adipocyte differentiation by modulating adipogenic genes. BMC Complement Altern Med. 2010. 10:34. https://doi.org/10.1186/1472-6882-10-34
Pak E, Segal RA. Hedgehog signal transduction: Key players, oncogenic drivers, and cancer therapy. Dev Cell. 2016. 38: 333-344.
Petricci E, Manetti F. Targeting the Hedgehog signaling pathway with small molecules from natural sources. Curr Med Chem. 2015. 22:4058-4090.
Pompeu DR, Pissard A, Rogez H, Dupont P, Lateur M, Baeten V. Estimation of phenolic compounds and antioxidant capacity in leaves of fruit species using near-infrared spectroscopy and a chemometric approach. BASE. 2021. 25:109-119.
Qiu S, Cho JS, Kim JT, Moon JH, Zhou Y, Lee SB, et al. Caudatin suppresses adipogenesis in 3T3-L1 adipocytes and reduces body weight gain in high-fat diet-fed mice through activation of hedgehog signaling. Phytomedicine. 2021. 92:153715. https://doi.org/10.1016/j.phymed.2021.153715
Rallu F, Gruss A, Maguin E. *Lactococcus lactis* and stress. Antonie Van Leeuwenhoek. 1996. 70:243-251.
Re R, Pellegrini N, Proteggente A, Pannala A, Yang M, Rice-Evans C. Antioxidant activity applying an improved ABTS radical cation decolorization assay. Free Radic Biol Med. 1999. 26:1231-1237.
Rosen ED, Hsu CH, Wang X, Sakai S, Freeman MW, Gonzalez FJ, et al. C/EBPα induces adipogenesis through PPARγ: a unified pathway. Genes Dev. 2002. 16:22-26.
Rosen ED, MacDougald OA. Adipocyte differentiation from the inside out. Nat Rev Mol Cell Biol. 2006. 7:885-896.
Sakuma S, Yabuuchi M, Yoshizumi A, Okajima Y, Fujimoto Y, Okuhira K. Comparative effects of luteolin and quercetin on adipogenesis in 3T3-L1 cells. J Pharmacy Nutr Sci. 2021. 11: 65-72.
Shao Y, Sun Y, Li D, Chen Y. *Chrysanthemum indicum* L.: A comprehensive review of its botany, phytochemistry and pharmacology. Am J Chin Med. 2020. 48:871-897.
Shraim AM, Ahmed TA, Rahman MM, Hijji YM. Determination of total flavonoid content by aluminum chloride assay: A critical evaluation. LWT. 2021. 150:111932. https://doi.org/10.1016/j.lwt.2021.111932
Skoda AM, Simovic D, Karin V, Kardum V, Vranic S, Serman L. The role of the Hedgehog signaling pathway in cancer: A comprehensive review. Bosn J Basic Med Sci. 2018. 18:8-20.
Song AA, In LLA, Lim SHE, Rahim RA. A review on *Lactococcus lactis*: from food to factory. Microb Cell Fact. 2017. 16:55. https://doi.org/10.1186/s12934-017-0669-x
Souza EC, Azevedo POS, Domínguez JM, Converti A, Oliveira RPS. Influence of temperature and pH on the production of biosurfactant, bacteriocin and lactic acid by *Lactococcus lactis* CECT-4434. CYTA J Food. 2017. 15:525-530.
Suh JM, Gao X, McKay J, McKay R, Salo Z, Graff JM. Hedgehog signaling plays a conserved role in inhibiting fat formation. Cell Metab. 2006. 3:25-34.
Wang J, Zhang W, Wang S, Wang Y, Chu X, Ji H. *Lactobacillus plantarum* Exhibits antioxidant and cytoprotective activities in porcine intestinal epithelial cells exposed to hydrogen peroxide. Oxid Med Cell Longev. 2021a. 2021:8936907. https://doi.org/10.1155/2021/8936907
Wang Q, Sun J, Liu M, Zhou Y, Zhang L, Li Y. The new role of AMP-activated protein kinase in regulating fat metabolism and energy expenditure in adipose tissue. Biomolecules. 2021b. 11:1757. https://doi.org/10.3390/biom11121757
Xu H, Hong JH, Kim D, Jin YH, Pawluk AM, Mah JH. Evaluation of bioactive compounds and antioxidative activity of fermented green tea produced via one- and two-step fermentation. Antioxidants. 2022. 11:1425. https://doi.org/10.3390/antiox11081425
Zebisch K, Voigt V, Wabitsch M, Brandsch M. Protocol for effective differentiation of 3T3-L1 cells to adipocytes. Anal Biochem. 2012. 425:88-90.
Zhang W, Lu J, Feng L, Xue H, Shen S, Lai S, et al. Sonic hedgehog-heat shock protein 90β axis promotes the development of nonalcoholic steatohepatitis in mice. Nat Commun. 2024. 15:1280. https://doi.org/10.1038/s41467-024-45520-8
Zhou Y, Kim JT, Qiu S, Lee SB, Park HJ, Soon MJ, et al. 1,3,5,8-Tetrahydroxyxanthone suppressed adipogenesis via activating Hedgehog signaling in 3T3-L1 adipocytes. Food Sci Biotechnol. 2022. 31:1473-1480.
Zielinska-Blizniewska H, Sitarek P, Merecz-Sadowska A, Malinowska K, Zajdel K, Jablonska M, et al. Plant extracts and reactive oxygen species as two counteracting agents with anti- and pro-obesity properties. Int J Mol Sci. 2019. 20:4556. https://doi.org/10.3390/ijms20184556
Zou Z, Wang H, Zhang B, Zhang Z, Chen R, Yang L. Inhibition of Gli1 suppressed hyperglycemia-induced meibomian gland dysfunction by promoting pparγ expression. Biomed Pharmacother. 2022. 151:113109. https://doi.org/10.1016/j.biopha.2022.113109